Dynamic Characteristic Identification on Steel Column bases Installed in Pendulum-type Earthquake Response Observatory

Choi Jae-hyouk*, Ohi Kenichi
Department of Architecture and Civil Engineering, Kobe University, 1-1 Rokodai-cho, Nada-ku, Kobe, 657-8501, Japan

An observatory termed 'Steel Swing' has been developed, where a 15000 kg pendulum is hanged from a stiff steel frame. A building element can be tested after inserted between the pendulum and the frame. Free vibration, forced vibration tests and earthquake monitoring were performed on an exposed-type steel column base. The response records monitored during natural earthquakes were used to identify the vibration property of the specimen. Identified system gain was approximated by a theoretical gain of linear SDOF system, and the response calculated based on such a linear system agrees with the monitored response fairly well. This research technique can be applied to check the behaviors of new materials and new details of connections and the safety of non-structural elements as well.

Key Words : Dynamic Characteristic, Free Vibration, Forced Vibration, System Gain, Single Degree of Freedom Viscous Damped System (SDOF)

1. Introduction

To estimate seismic behavior of the structure with accuracy, an earthquake response observation device (Steel Swing) is developed and the possibility of its application is investigated. Free vibration, forced vibration tests and earthquake monitoring were carried out to study the dynamic properties of an exposed-type column base. From the results of these tests, dynamic properties of the exposed-type column base including natural frequencies, damping ratios and initial rotation stiffness are presented. Furthermore, transmission characteristic of the system is identified using observed acceleration records. Steel Swing is set up at Chiba experiment station in Institute of Industrial Science (IIS), University of Tokyo in Japan. When an earthquake occurs, movement of the pendulum, which is hanged on the observatory structure, provides an inertial force to specimen, which is inserted between pendulum and observatory structure. By applying an excitation force to the pendulum, collapse process of the building elements can be observed and its dynamic characteristics can be measured. Free vibration, forced vibration tests and earthquake monitoring were carried out to study the dynamic properties of an exposed-type column base, system identification techniques using Fast Fourier Transformation are applied to the observed acceleration records.

* Corresponding Author,
E-mail : jhchoi@kobe-u.ac.jp
TEL : +81-90-3526-4556; **FAX** : +81-78-803-6048
Department of Architecture and Civil Engineering, Kobe University, 1-1 Rokodai-cho, Nada-ku, Kobe, 657-8501, Japan. (Manuscript **Received** September 6, 2004; **Revised** September 29, 2004)

2. Outline of Earthquake Response Observation Device

2.1 The aim of the device

The Steel Swing is set up at the Chiba experiment station in Institute of Industrial Science (IIS), University of Tokyo (Jul, 2001). When an earthquake occurs, movement of the pendulum, which is hanged on the observatory structure, provides an inertial force to building element. A

building element is inserted between the pendulum and the observatory structure. By applying an excitation force to the pendulum, the collapse process of the building elements can be observed and its dynamic characteristics can be measured.

As the same test scheme, there is a test example using the shaking table (Akiyama, 1998). By applying an inertia force to the specimen, which is generated by shaking mass, collapse process of the building elements have been observed. However, the cost of using the shaking table is expensive. On the other hand, this pendulum type earthquake observation device, can achieve economical experiments since the natural excitation of the ground is used. Furthermore, forced resonance vibration tests can also be carried out easily by using a vibration excitation device indoors. Exchange of specimen is comparatively convenient.

2.2 Detail of steel swing

The performance of steel swing is shown in Table 1. Although a pendulum with 150 kN mass is hanged at the present state, this mass of pendulum can be increased to maximum 300 kN. The length of the steel bar, which carries the pendulum, is 243 cm and this length can be increased to maximum 263 cm. The period of the pendulum is 3.13 sec in the natural state. It becomes approximately 1 second if supported by specimens, which is inserted between the pendulum and the observatory structure, as shown in Fig. 1. Plan of steel swing is presented in Fig 2. The calculated stiffness of observatory device is 19500 kN/m in strong axis and 4500 kN/m in weak axis. They correspond to 0.075 sec and 0.16 sec of calculated period, respectively. Since the mass of the pendulum can be changed up to 300 kN, the applied force to the test setup can be adjusted. Furthermore, since the joints are suspended by universal joint, which can move in x and y-axis freely, horizontal bi-axial response of the steel swing can be observed, and the force actually applied to the building elements is reproducible. Four steel suspension bars with turnbuckle resist of the axial force.

Table 1 Specification for pendulum

Mass of pendulum	Present 1500 kN (Max. 3000 kN)
The length of steel bar	Present 2.43 m (Max. 2.63 m)
Period (Without specimen)	3.13 Sec
Period (With specimen)	0.95-1.03 Sec

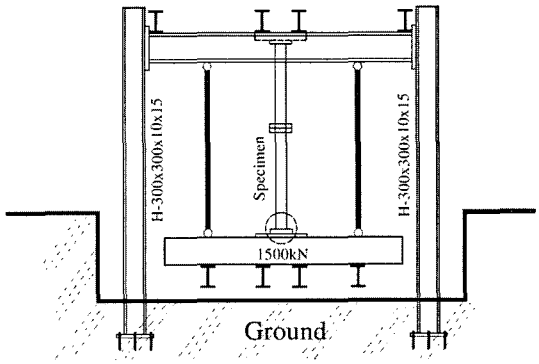

Fig. 1 Earthquake response observation devices 'Steel Swing'

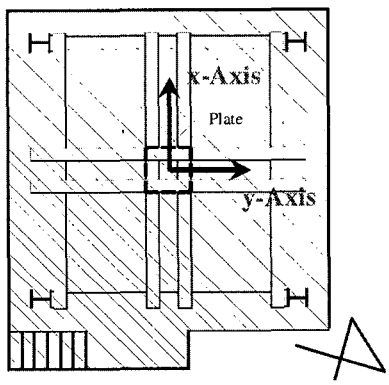

Fig. 2 Plan of steel swing

3. Free Vibration and Forced Vibration Tests

3.1 Detail of specimen

The specimen of the exposed-type steel column base is shown in Fig. 3. The square hollow steel column □50×150×6 is used in the experiment, and the diameter of the anchor bolts was 12 mm

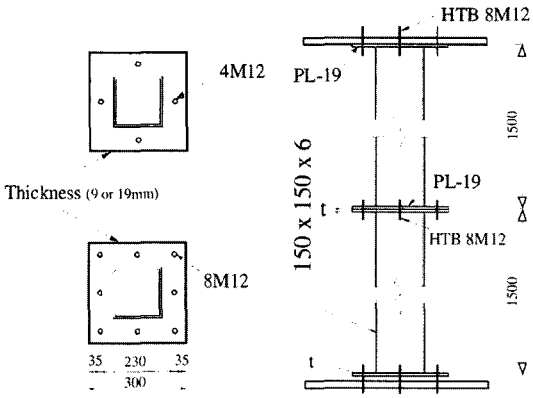

Fig. 3 Dimensions of column base specimen

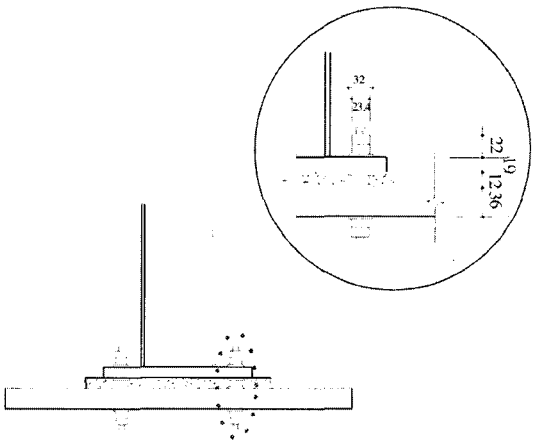

Fig. 4 Detail of specimen with mortar

all with screw. The specimens were fabricated and fixed rigidly to the rigid foundation. To achieve contact with the foundation surface, high strength, non-shrinkage mortar was grouted. The test set-up is prepared by considering the distribution of anchor bolts and base plate thickness. The variable parameters in the tests were thickness of the base plates, number of anchor bolts as shown in Table 2. As shown in Fig. 4, by placing ordinary mortar of thickness 12 mm between base plate and the supporting plate, anchor bolts are installed. To prevent loosen of anchorage of anchor bolts double nut is installed. The material of base plate and anchor bolts is JIS SS400 (Table 3).

3.2 Measuring plan of test

The response data of the observatory structure,

Table 2 Tests code for the vibration tests

Thickness of Base plate	Arrange of Bolt	Free Vibration test	Forced vibration test
19mm	8	FRV19m8	FOV19m8
19mm	4	FRV19m4	FOV19m4
9mm	8	FRV 9m8	FOV 9m8
9mm	4	FRV 9m4	FOV 9m4
Without specimen		FRV Pendm	—

Note ; FRV stands for 'FRee Vibration test' and FOV stands for 'FOrce Vibration test'.

Table 3 Material test result of base plate

	σ_y (N/mm^2)	σ_u (N/mm^2)	σ_y/σ_u (%)	EL (%)
B.PL 9 mm	274.4	450.0	61	18
B.PL 19 mm	245.0	421.4	58	18

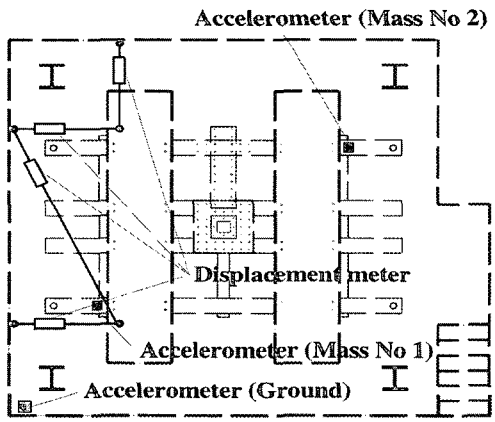

(a) Plan

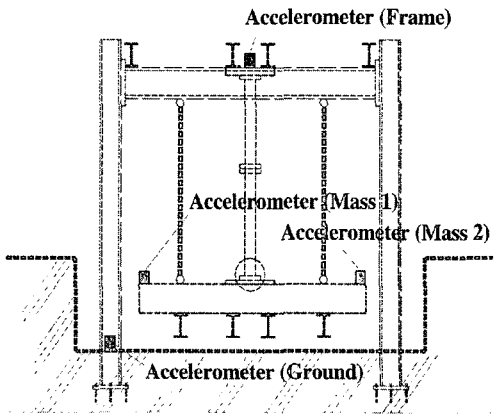

(b) Elevation

Fig. 5 Measuring arrangements for steel swing

test specimen and the ground were recorded as digital quantities using sampling period of 1/200 sec. The data acquisition is automatically started once 5 gal is sensed at the basement, and data are converted into the digital form every sample time. The following global accelerations were measured using accelerometers horizontally (x and y axis) (Fig. 5(a)). (1) At the basement (2) On the pendulum (3) At the top portion of the observatory frame. The displacements at the corner of pendulum are measured by using 4 displacement meters, as shown in Fig. 5(b). In order to measure flexural strains on the column member, 8 strain gages are attached to both lower and upper parts of the column. The measurement system has a 22-channel simultaneous measurement and data acquisition capacity. This device is not taken into consideration to a motion of the vertical direction.

3.3 Outline of free vibration test

In order to understand the dynamic characteristics of exposed-type column base, free vibration test is carried out in elastic range. During the free vibration test, the load is applied to the center of the pendulum by manpower and it is made to vibrate freely. To stay in elastic range, the later load is applied to lower than 1/150 rad of member rotation angle.

3.4 Forced vibration test using excitation device

In these tests, a counter-rotating eccentric-weight-type vibration excitation device was set up at the center of the pendulum. Forced vibration tests including the phased sweep tests were performed in the direction of strong axis. The vibration excitation device properties are shown in Table 4.

The maximum force of the vibration excitation device was 10 kN, and the exciting range was 2.5-50 Hz. During the tests, sine cycles with several cycle (frequency) numbers are applied to the specimen in its elastic range.

Table 4 Specifications for excitation device

Excitation type	Counter-rotating eccentric-weight-type
Excitation direction	Horizontal and vertical direction
Excitation cycle	Sine cycles
Maximum force	10 kN
Excitation moment	5 N·m
Range of excitation	2.5-50 Hz

3.5 Summary of free and forced vibration test result

3.5.1 Test result of free vibration test

Dynamic properties of the system are discussed using the records obtained from the free vibration test. The system is excited harmonically at its fundamental resonance frequency by manpower. Table 5 shows the natural frequencies and damping factors for the free vibration tests. The natural frequency could be seen before and after 1 Hz

Table 5 Summary of free vibration test results

Test code	Period of strong axis (Sec)	Stiffness (kN/m)	Damping factor
FRV19m8	0.95	729	0.0048
FRV19m4	0.96	714	0.0039
FRV9m8	1.00	658	0.0040
FRV9m4	1.03	620	0.0040
FRV Pendm (without specimen)	3.0	—	

Note; FRV stands for 'FRee Vibration test' and FOV stands for 'FOrce Vibration test'.

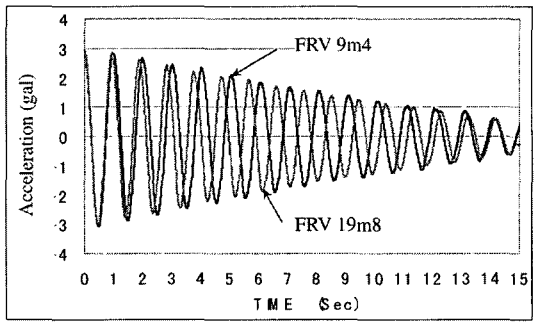

Fig. 6 Time histories of acceleration recorded in free vibration tests

in all specimens. Free vibration test result is shown in Fig. 6. In case of thin base plate and 4-bolt type, the rigidity was the lowest. For this reason, the frequency becomes longer. On the other hand, even if the vibration frequency of the test specimen is different, it is not observed that the hyperbolic curve of damped oscillation is approximately the same. As shown in Fig. 7 the

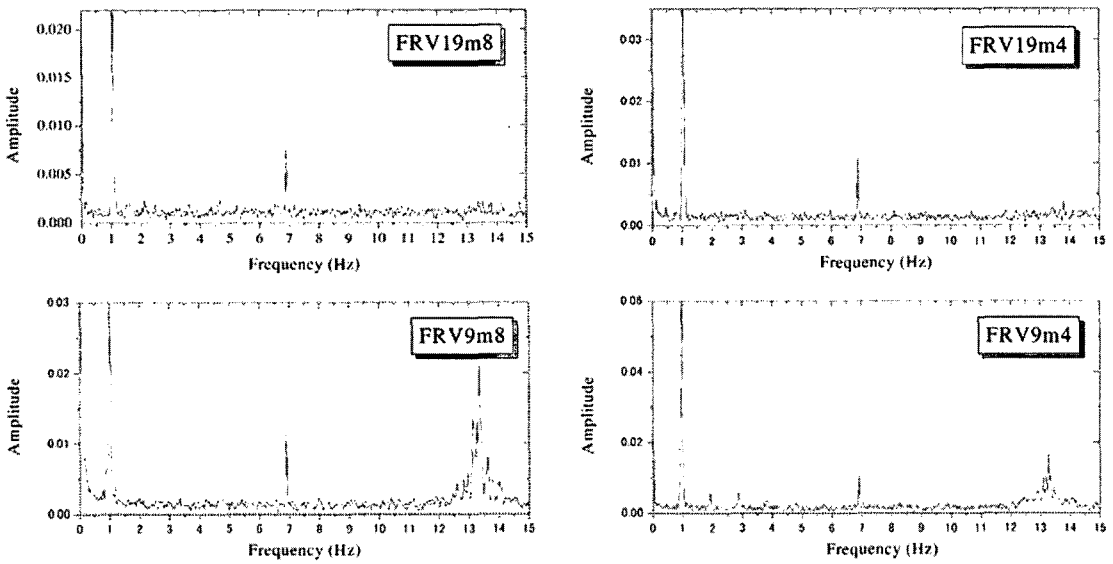

Fig. 7 Fourier amplitude spectra derived from free vibration test on the observatory structure

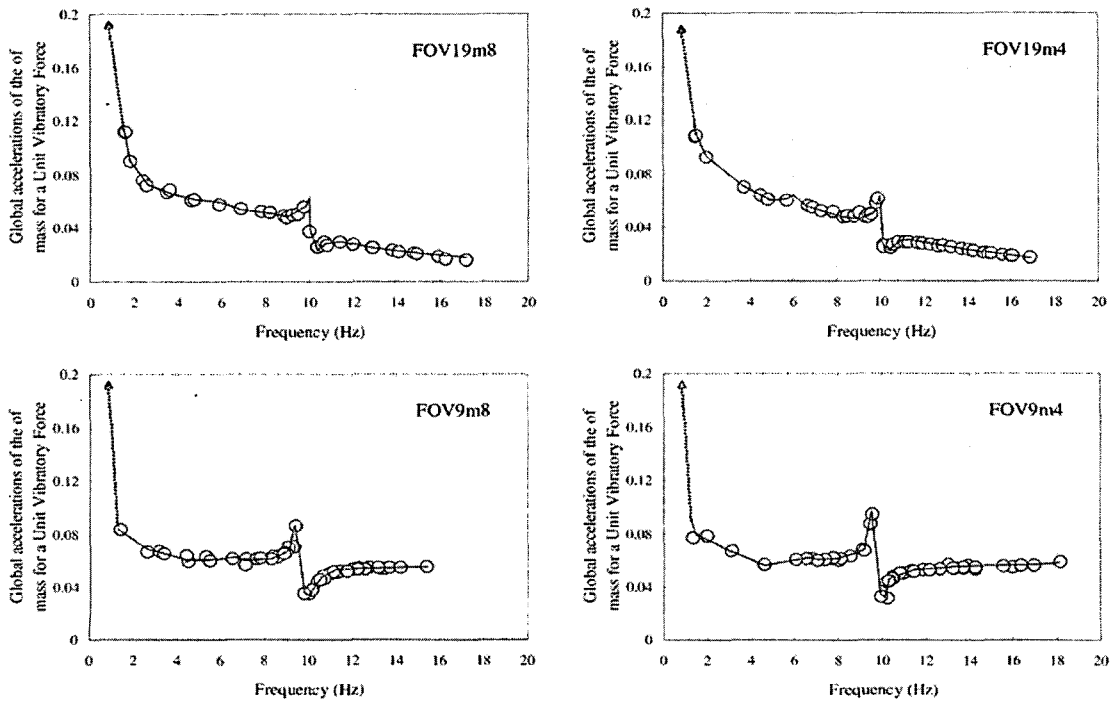

Fig. 8 Resonance curve observed on the pendulum

first peak is natural frequency of mass. The second and third-peak correspond to natural frequency of observatory structure of weak and strong axis.

3.5.2 Test results of forced vibration test

Sweep excitation test is carried out by the vibration excitation device. The mass was excited in y-axis, which is strong axis of this system. Fig. 8 shows the results of test observed on the mass and Fig. 9 shows the results of test observed on top of the observatory structure respectively. In these figures, the vertical axis indicates the global acceleration of the mass for a unit vibratory force. In case of forced resonance test, it is limited at the check of the secondary and third resonance point, because the first resonance point is exceeded the limit of the possible frequency region of vibrate excitation device. It is clear from forced vibration test that for this device 9.5 Hz and 13 Hz of 2nd and 3rd modes are taken as resonance points, respectively. According to the vibration of the beam supporting the upper part of the observatory structure, it is suggested that this device should be considered as 2 different concentrated masses. For the reasons given above, it should be concluded that the device needs to remove high frequency component using a low pass filter and to strengthen at the top portion and weak axis of the device.

3.5.3 Comparison of elastic rotation stiffness

The connection between the steel column base and the concrete foundation has a rotational rigidity significant for the overall frame analysis. This rigidity could be taken into account to predict the horizontal drift of the frame in serviceability limit state. The comparison of the values obtained from the test and calculation of the elastic rotation stiffness is presented in Table 6. The elastic rotation stiffness of each test specimen is derived from the free vibration tests. This value is obtained by extracting stiffness of column from the elastic rotation stiffness of column base. The formula of elastic rotation stiffness of exposed-type column base was already suggested in Recommendation for Limit State Design of Steel Structures of AIJ. However this formula cannot take inner bolts into consideration. When inner bolts are also considered, the calculation elastic rotation stiffness is derived (Appendix (A)). Mechanical model of column base is presented in Fig. A. On the other hand, when the applied lateral force to the column base, deformation is occurred not only the elongation of anchor bolts but also the out of plane deformation of base plate. The model, which is consi-

Table 6 Comparison of the rotation stiffness (kN·m/rad)

	${}_eK_\theta$	${}_cK_\theta$	${}^{**}{}_cK_\theta$	${}^{*}{}_cK_\theta/{}_eK_\theta$	${}^{**}{}_cK_\theta/{}_eK_\theta$
19mm8	21364	16187	32299	0.75	1.5
19mm4	19987	6484	17587	0.32	0.88
9mm8	15803	18980	11067	1.20	0.70
9mm4	13583	7597	9197	0. 56	0. 68

${}_eK_\theta$ Test value, ${}^{*}{}_cK_\theta$ Reference (AIJ/LSD), ${}^{**}{}_cK_\theta$ Reference (K. Masuda)

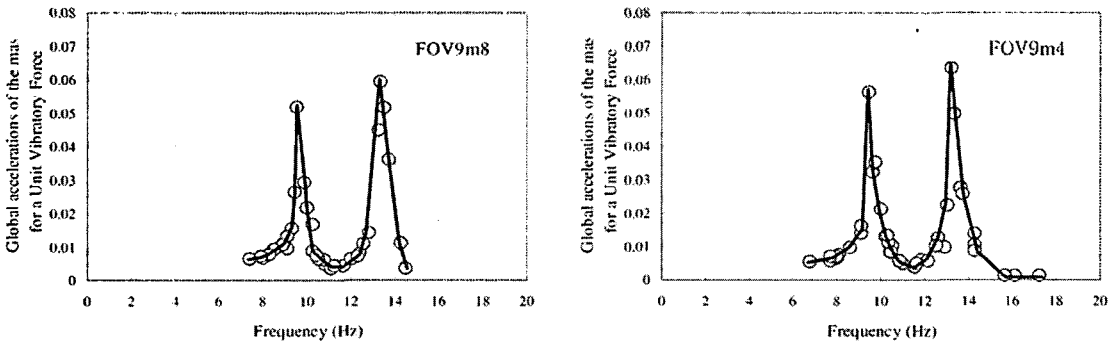

Fig. 9 Resonance curve observed on the top of the observatory structure (9 mm base plate)

dered the out of plane deformation of base plate, is derived to be compatible with the rotation stiffness of test result in Fig. B (Appendix (B)). According to the comparison, calculated value of the rotation stiffness, which considers the out of plane deformation of the base plate also, is more close to the experimental value compared with the AIJ/LSD (1998).

4. Elastic Response Observation of a Real Earthquake

4.1 Summary of observed earthquake response

Observed earthquake response data are summarized in Table 7.

4.2 Spectral analysis of transfer characteristics

The FFT techniques are utilized in order to identify the spectral characteristics of the system. The data processing in the system identification was carried out in the following way: Consider the unknown system, whose input and output time series are denoted by $x(t)$ and $y(t)$, respectively. The Fourier transforms of these time series, $X(\omega)$ and $Y(\omega)$, can be approximated by the finite complex Fourier components in the FFT computation. The energy spectrum or the fourier square amplitude spectrum of the input time series, denoted by S_{xx}, and the cross spectrum of the input and out-put time series, denoted by S_{xy}, are calculated under the following definitions:

$$S_{xx}=X^*(\omega)\,X(\omega) \tag{1}$$

$$S_{xy}=X^*(\omega)\,Y(\omega) \tag{2}$$

where, $X^*(\omega)$ denoted the conjugate of $X(\omega)$.

Evidently, S_{xx} and S_{xy} indicate the contribution of each spectral component to the two integrals $\int(x(t))^2dt$ and $\int(x(t)\ y(t))\,dt$, respectively. Although some smoothing techniques are used to make no change in the original value of the two integrals $\int(x(t))^2dt$, it may remove peak point of the original value. The acquisition technique is explained in the next section, in detail. The obtained energy spectrum and the obtained cross spectrum are denoted by $\overline{S_{xx}}$ and $\overline{S_{xy}}$, respectively. The system function of this

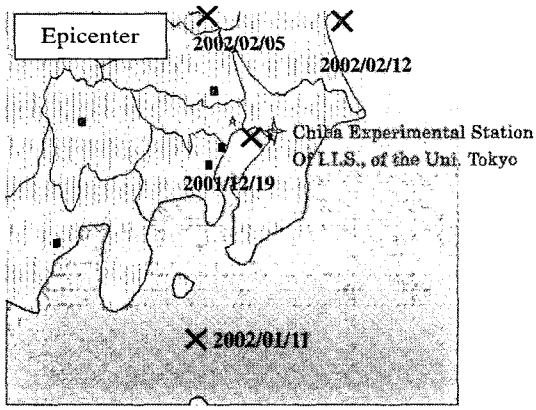

Fig. 10 Location of epicenter and monitoring site

Table 7 Measurement earthquake data

Measurement date	Epicenters	Magnitude depth distance of epicenter	Maximum acceleration (cm/sec²)			
			Basement x	Mass x	Basement y	Mass y
19 Dec. 2001 00:07	N.Lat 35.2 E.Long 139.5	M4.0 100 Km	4.1	2.1	3.3	2.3
1 Jan. 2002 00:41	N.Lat 34.2 E.Long 139.7	M4.7 110 Km	4. 3	4. 4	2. 1	4. 4
5 Feb. 2002 19:57	N.Lat 36.3 E.Long 140.0	M4.4 70 Km	2.5	1.5	4	1.25
12 Feb. 2002 22:44	N.Lat 36.6 E.Long 141.0	M5.5 40 Km	10	8.1	7.5	15

input-output system, denoted by $H(\omega)$, is defined as a complex function, which satisfies the following equation:

$$Y(\omega)=H(\omega)X(\omega) \tag{3}$$

The system function $H(\omega)$ can be identified by:

$$|H(\omega)|=\frac{|S_{xy}(\omega)|}{S_{xx}(\omega)} \tag{4}$$

Four observed acceleration records, which are recorded at the foundation of observatory structure for each earthquake, are chosen to identify system. Obtained Fourier amplitude spectra of the above mentioned records and the system gain are shown in Fig. 14.

4.3 The approach solving spectral values essentially

The FFT techniques have high resolving capacity, but the computed spectral values often show abrupt changes, which may be caused by some errors included in the data. Generally, in order to remove these unstable changes and to pay attention to slowly changed essentials, some

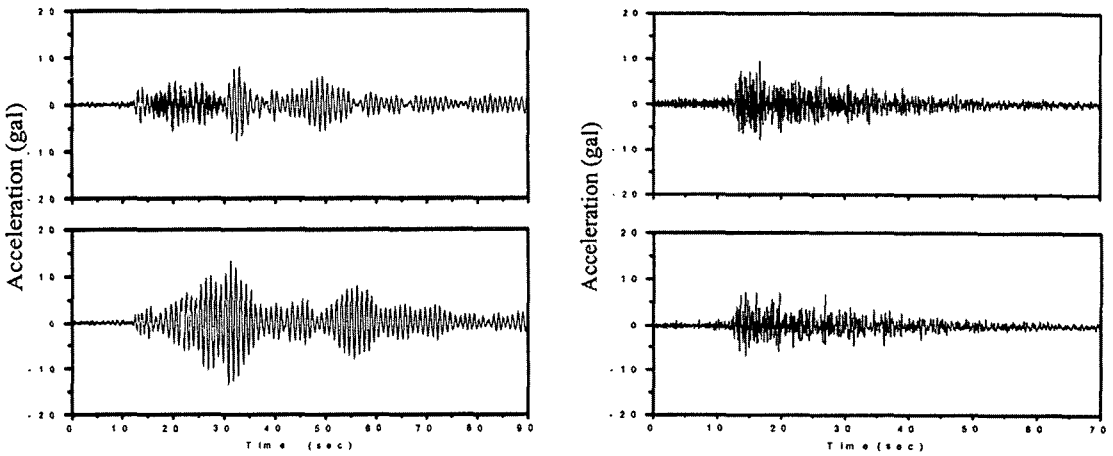

(a) Basement (b) Pendulum

Fig. 11 Time history of acceleration (12 Feb. 2002) (Up :d x-axis, down : y-axis)

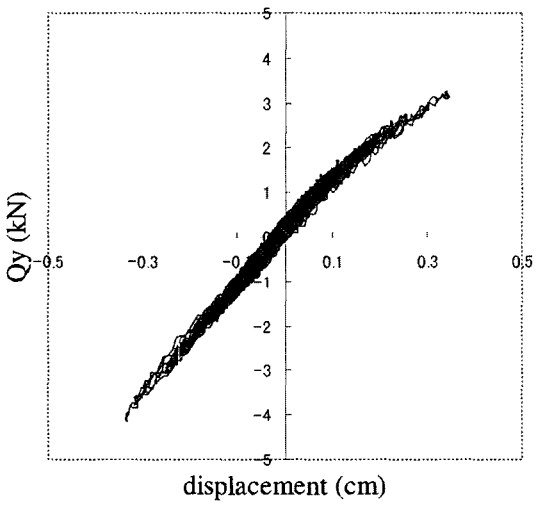

Fig. 12 Hysteresis loops (12 Feb. 2002)

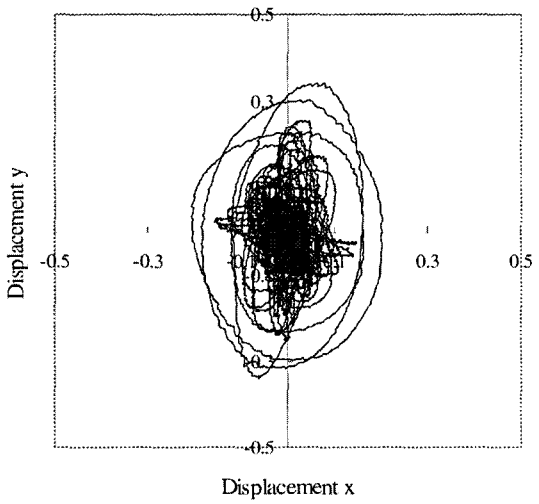

Fig. 13 Displacement response paths (12 Feb. 2002)

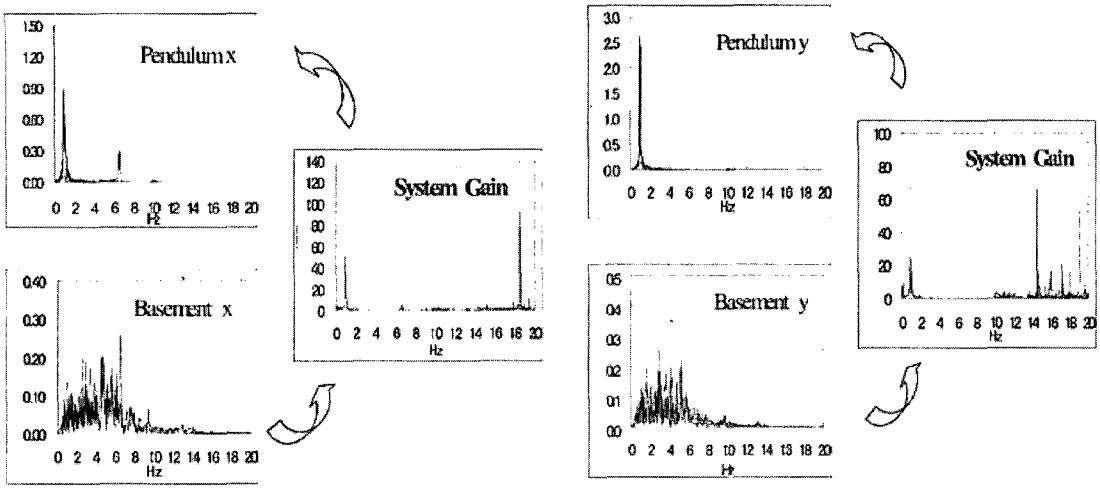

Fig. 14 System gain (12 Feb. 2002)

smoothing techniques are applied to the spectral values. There are many kinds of smoothing techniques such as : Rectangular spectral window, Bartlett spectral window, Parzen spectral window, Hanning spectral window, and Hamming spectral window techniques. However, it is possible that the peak of original value is removed using a smoothing technique. For reasons mentioned above, in this section, the spectral values, S_{xx} and S_{xy}, are calculated by assembly of average value without doing any smoothing. The average value is obtained from averaging 100 spectral values with 0.005-sec time intervals.

4.4 Verification of the identification of system gain (12 Feb. 2002)

The identified system gain was compared with the theoretical system gain of Single Degree of Freedom Viscous Damped System (Fig. 15), which adjusts the parameter in Fig. 16.

The theoretical system gain is derived from the following formula.

$$|System\ gain| = \frac{\sqrt{\omega_0^4 + 4h^2\omega_0^2\omega^2}}{\sqrt{(\omega_0^2 - \omega^2)^2 + 4h^2\omega_0^2\omega^2}} \quad (5)$$

In order to confirm the validity of identified dynamic characteristic, earthquake response analysis is performed in the time domain by the model of Single Degree of Freedom Viscous Damped System, and it was compared with the time history of an observation result for the data of 12 Feb. 2002 in Fig. 17.

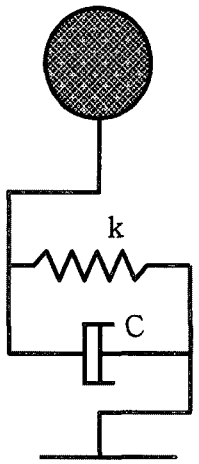

Fig. 15 Model of SDOF system

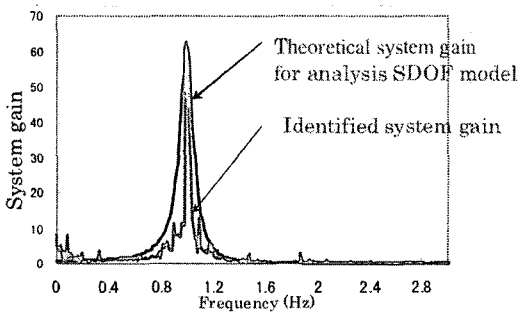

Fig. 16 Identification of transfer characteristic

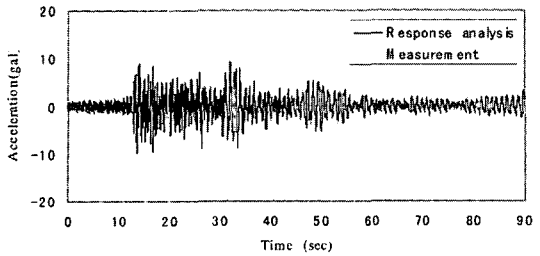

(a) x-axis

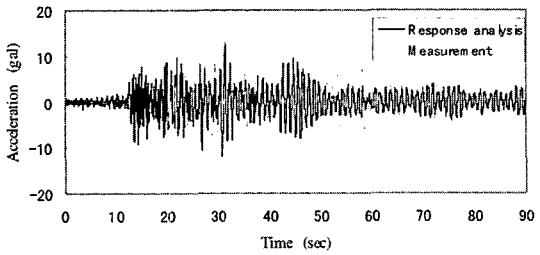

(b) y-axis

Fig. 17 Response time histories of x-axis

5. Conclusion

An earthquake response observation device (Steel Swing) is developed and the possibility of its application is examined. Free vibration, forced vibration tests and natural earthquake measurement on an exposed-type column base using a steel swing were carried out. From the test results, it was found that the device needs to remove high frequency component using a low pass filter and to strengthen at the top portion and weak axis of the device. It is observed that natural frequencies were different due to the number of anchor bolts and the thickness of base plate. However the damping factors were nearly the same.

An outline of elastic response due to earthquakes has been described. The data acquisition system works well, and natural earthquake responses of system have been successfully recorded. System identification techniques using Fast Fourier Transform are applied to the observed acceleration records. Identified system gain was approximated by a theoretical gain of linear SDOF system, and the response calculated based on such a linear Single degree of freedom viscous damped system agrees with the monitored response fairly well. This research technique can be applied to check the behaviors of new materials and new details of connections. By using the simple vibration model, which suits identified transfer characteristics, it turns out that the earthquake response can be regenerated.

References

AIJ, 1998, "Recommendation for Limit State Design of Steel Structures".

Akiyama, H., 1998, "The Scheme of the Real Scale Shaking Table Test for the Structural Members Using the Inertia Force," *Journal of Struct*, Constr, Engng, AIJ, No. 505, pp. 139~146.

Hagiwara, Y., Akiyama, H., Kokubo, K. and Sawada, Y., 1991, "Post-Buckling Behavior During Earthquake and Seismic Margin of FBR Main Vessels," *Int. J. Res. & Piping 45*, pp. 259~271.

Kanshi Masuda, 1980, "Experimental Studies on Mechanical Characteristics of The Steel Column Bases (Part 1 : Deformation behaviour of Column bases subjected to bending moment), Journal of Structural and Construction Engineering (Transaction of AIJ)," Vol. 297.

Kenichi Ohi and Koichi Takanashi, 1987, "Response Observation of Weekly Designed Steel Structure Models," *J. Structure Engineering*, Vol. 33B.

Koichi Takanashi and Kenichi Ohi, 1987, "Response Observation of Scaled Model Structures to Strong Earthquakes," *J. Construct. Steel Research*, Vol. 13.

Memari, A. M., Aghakouchak, A. A., Ghafory M. Ashtiany and Tiv, M., 1999, "Full-scale Dynamic Testing of a Steel Frame Building During Construction," *Engineering Structures*, ELSEVIER, 21, pp. 1115-1127.

Meng, K., Ohi, K. and Takanashi, K., 1992, "A simplified Model of Steel Structural Members with Strength Deterioration used for Earthquake Response Analysis," *Journal of Struct. Constr.* Engng, AIJ, No. 437, pp. 115~124.

Nishida, A., Ohi, K., Kondo, H., Shimawaki, Y., Lin, X. G., Miyama, T. and Yamashita, S., 1996, "Vibration tests on a 3-story Steel Building

Model with Hysteresis Dampers," Bull. ERS, No. 29.

Ohi, K., Tanaka, H. and Takanashi, K., 1985, "A Simple Method to Estimate the Statistical Parameters of Energy Input to Structures during Earthquakes," *Journal of Struct*, Constr, Engng, AIJ, No. 347, pp. 47~55.

Appendix

Elastic rotation stiffness of Exposed-type Column base.

(A) Not considers the out of plane deformation of the base plate (AIJ/LSD)

$$K_\theta=\frac{E_s\cdot A_b}{2\cdot l_b}\{n_1\cdot(d_t+d_c)^2+n_2\cdot d_c^2\} \qquad (A)$$

Where,

E_s: Modulus of elasticity of steel
A_b: Effective section area of anchor bolts
n_1 : Number of outer bolts
n_2 : Number of inner bolts
d_t : The distance from centroid of column to anchor bolt of tensile side
d_c : The distance from centroid of column to under of column flange
l_b : Effective length of anchor bolt

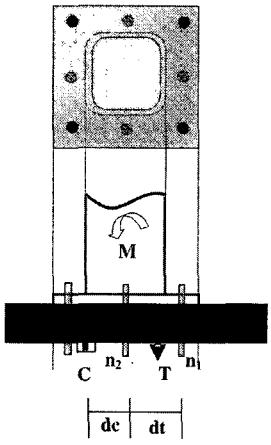

Fig. A Mechanical model of column base (AIJ/LSD)

(B) Considers the out of plane deformation of the base plate (Masuda, 1980)

$$K_\theta=K_{b1}\left(l_1-\frac{x_n}{3}\right)(l_1-x_n)+K_{b2}\left(l_2-\frac{x_n}{3}\right)(l_2-x_n)$$

$$\frac{1}{k_{b1}}=\frac{l_b}{n_1E_sA_b}=\frac{(a_1-s)^3}{3E_sI_{P1}} \qquad (B)$$

$$\frac{1}{k_{b2}}=\frac{l_b}{n_2E_sA_b}+\frac{(a_1-s)^3}{3E_sI_{P2}}$$

$$I_{P1}=\frac{D\cdot t^3}{12},\ I_{P2}=\frac{(l_1-x_n-a_1)\cdot t^3}{12}$$

Where,

X_n: The location of neutral axis

$$x_n=\frac{n\cdot A_b(n_1+n_2)}{D}\cdot\left\{-1+\sqrt{1+\frac{2D}{(Es/Ec)\cdot A_b}\left(\frac{n_1l_1+n_2l_2}{n_2+n_2}\right)}\right\}$$

E_s/E_C : Ratio of Modulus of elasticity

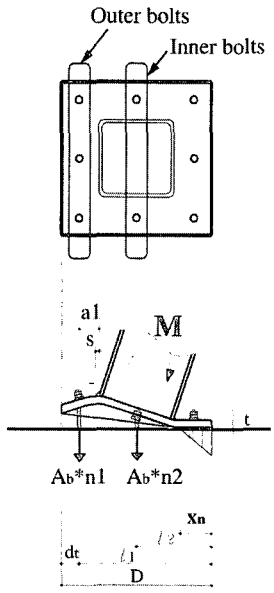

Fig. B Mechanical model of column base (K. Masuda)